Journal of Organometallic Chemistry, 408 (1991) 77–94
Elsevier Sequoia S.A., Lausanne
JOM 21604

Cluster chemistry

LXVII *. Reactions of some Fe–Ir clusters. Crystal structures of $Fe_2Ir(\mu\text{-}H)(\mu_3\text{-}CCHPh)(CO)_8(PPh_3)$ and $Au_2Fe_2Ir(\mu_4\text{-}C_2Ph)(CO)_7(PPh_3)_3$

Michael I. Bruce, George A. Koutsantonis and Edward R.T. Tiekink

Jordan Laboratories, Department of Physical and Inorganic Chemistry, University of Adelaide, Adelaide, South Australia 5001 (Australia)

(Received October 5th, 1990)

Abstract

Isomeric hydrido-vinylidene and -alkyne complexes $Fe_2Ir(\mu\text{-}H)(\mu_3\text{-}X)(CO)_8(PPh_3)$ (X = CCHPh, HC_2Ph) were obtained from $Fe_2Ir(\mu_3\text{-}C_2Ph)(CO)_8(PPh_3)$ and H_2 or H^-/H^+. The X-ray structure of the vinylidene complex is reported. Cluster complexes containing gold, iron and iridium were obtained from $AuCl(PPh_3)$ or $[O\{Au(PPh_3)\}_3]^+$ and anionic species prepared from $Fe_2Ir(\mu_3\text{-}C_2Ph)(CO)_8(PPh_3)$. The mono-gold species $AuFe_2Ir(\mu_3\text{-}HC_2Ph)(CO)_8(PPh_3)_2$ and the tri-gold cluster $Au_3Fe_2Ir(C_2HPh)(CO)_7(PPh_3)_4$ were identified spectroscopically, whereas the digold complex $Au_2Fe_2Ir(\mu_4\text{-}C_2Ph)(CO)_7(PPh_3)_3$ was shown crystallographically to have an unusual structure in which one of the gold atoms bridges the acetylide C_α and the Ir atom. The rhodium analogue was also obtained.

Introduction

We have recently described the synthesis and characterisation of several mixed-metal clusters containing iron and iridium containing acetylide ligands [1]. In the course of developing their chemistry, we have compared the protonation and auration reactions of $Fe_2Ir(\mu_3\text{-}C_2Ph)(CO)_8(PPh_3)$ (**1**). The former yielded isomeric hydrido-alkyne and -vinylidene complexes. The aurating agents we have used included $AuCl(PPh_3)$ and $[O\{Au(PPh_3)\}_3]^+$, and a combination of the latter with $[ppn]^+$ salts, which we have found to be an excellent source of the $Au_2(PPh_3)_2$ group. This chemistry is described below, and amplifies in part a recent communication [2]. The complex $[PPh_4][AuFe_2Ir_2(CO)_{12}(PPh_3)]$, obtained from $[Fe_2Ir_2(CO)_{12}]^{2-}$ and $AuCl(PPh_3)$, has been described [3].

* For Part LXVI see ref. 1.

Results and discussion

Reactivity of $Fe_2Ir(\mu_3\text{-}C_2Ph)(CO)_8(PPh_3)$ (1)

(a) *With dihydrogen.* Reactions between **1** and H_2 in cyclohexane afforded the hydrido-vinylidene cluster $Fe_2Ir(\mu\text{-}H)(\mu_3\text{-}CCHPh)(CO)_8(PPh_3)$ (**2**) (Scheme 1), which is described in more detail below, and an unidentified brown complex which was obtained as the major product from a complex mixture.

(b) H^-/H^+. While the reaction between **1** and H_2 is complex, the two-stage addition of H^- (as $K[BH(CHMeEt)_3]$) and H^+ gave two well-defined products, **2** and the isomeric hydrido-alkyne derivative $Fe_2Ir(\mu\text{-}H)(\mu_3\text{-}HC_2Ph)(CO)_8(PPh_3)$ (**3**). These two complexes were also obtained by protonation of the anionic species formed by sodium amalgam-reduction of **1** in tetrahydrofuran. Both complexes were formulated from elemental microanalyses and their spectroscopic properties; the molecular structure of **2** was determined unambiguously by an X-ray diffraction study.

Structure of $Fe_2Ir(\mu\text{-}H)(\mu_3\text{-}\eta^2\text{-}CCHPh)(CO)_8(PPh_3)$ (2). The structure of **2** is shown in Fig. 1; significant bond distances and angles are given in Table 1. In the Fe_2Ir core, one Ir–Fe distance [Fe(1)–Ir 2.705(1) Å] is comparable to those in **1** [2]; the other [Fe(2)–Ir 2.656(1) Å] is considerably shorter. The Fe–Fe separation shows a significant lengthening compared with **1** (ca. 0.11 Å), suggesting that the hydride, which was not directly located, bridges this bond; this is supported by the 'splayed-out' nature of CO(5) and CO(6) about this bond. The PPh_3 and eight CO ligands are distributed as in the precursor **1**. The Ir–P(1) distance [2.362(1) Å] is unexceptional and similar to that in **1** [2.351(2) Å]. The μ_3-phenylvinylidene ligand interacts in a distorted η^2-fashion with Fe(2) [C(9)–Fe(2), C(10)–Fe(2) 2.806(4), 2.282(5) Å, respectively] while C(9) is attached to both Fe(1) [1.900(5) Å] and Ir [2.034(5) Å].

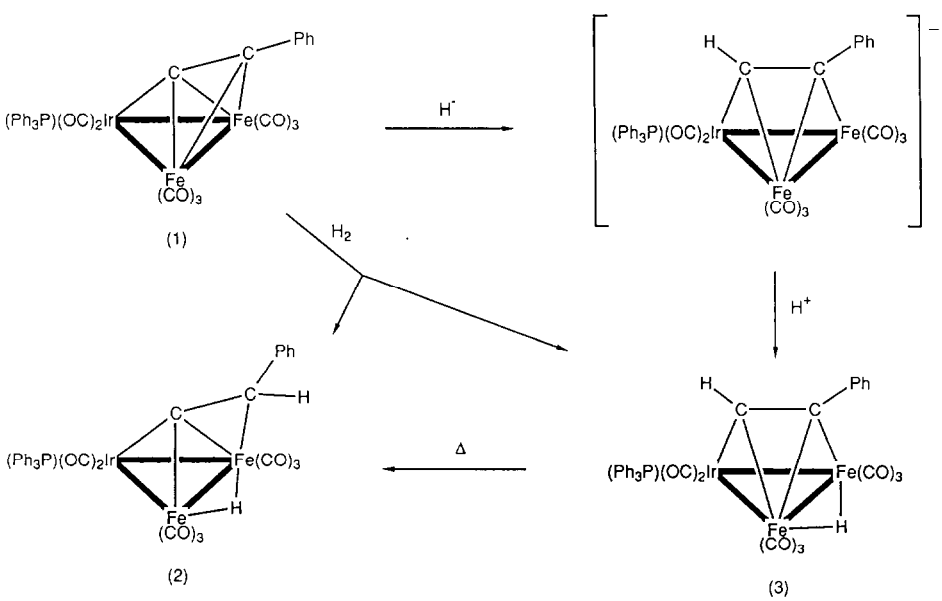

Scheme 1.

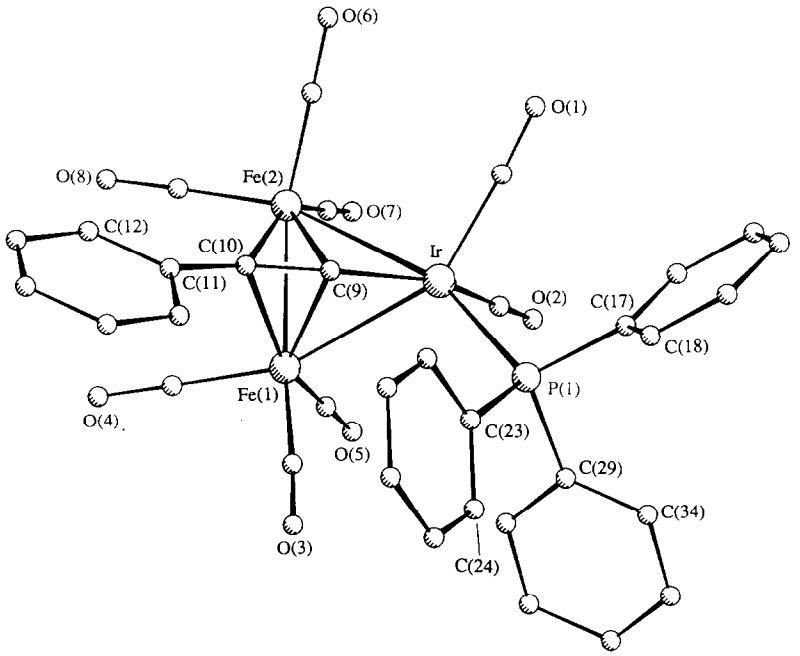

Fig. 1. Molecular structure and crystallographic numbering scheme for $Fe_2Ir(\mu\text{-}H)(\mu_3\text{-}CCHPh)(CO)_8(PPh_3)$ (**2**).

This type of structure in which the least electron-rich metal atom interacts with the C=C double bond, follows the pattern observed with other mixed-metal systems such as $Co_2Ru(\mu_3\text{-}CCHPh)(CO)_9$ [4]. The C(9)–C(10) distance [1.406(7) Å] has appreciably lengthened from that of the acetylide in **1**.

The spectroscopic properties in solution are consistent with the solid-state structure. The IR spectrum contains an eight-band terminal ν(CO) pattern. In the ^{1}H NMR spectrum, the vinylidene proton is found at δ 6.93, this signal is relatively broad, perhaps as a result of a small unresolved coupling to ^{31}P. The metal-bonded proton resonance is at δ −17.9 is coupled to both the vinylidene CH and the ^{31}P nucleus.

Table 1

Significant bond distances (Å) and angles (deg) in $Fe_2Ir(\mu\text{-}H)(\mu_3\text{-}CCHPh)(CO)_8(PPh_3)$ (**2**)

Ir–Fe(1)	2.705(1)	Ir–Fe(2)	2.656(1)
Fe(1)–Fe(2)	2.591(1)	Ir–P(1)	2.362(1)
Ir–C(9)	2.034(5)	Fe(1)–C(9)	1.900(5)
Fe(2)–C(9)	2.006(4)	Fe(2)–C(10)	2.282(5)
C(9)–C(10)	1.406(7)	C(10)–C(11)	1.492(6)
Fe(1)–Ir–Fe(2)	57.8(1)	Ir–Fe(1)–Fe(2)	60.2(1)
Ir–Fe(2)–Fe(1)	62.0(1)	P(1)–Ir–Fe(1)	106.4(1)
P(1)–Ir–Fe(2)	148.9(1)	Ir–C(9)–Fe(1)	86.8(2)
Ir–C(9)–Fe(2)	82.2(2)	Fe(1)–C(9)–Fe(2)	83.0(2)
C(9)–C(10)–Fe(2)	60.5(3)	C(9)–C(10)–C(11)	126.3(4)
Fe(2)–C(10)–C(11)	120.5(3)		

The ^{13}C NMR spectrum contained signals between δ 126–130 assigned to the phenyl protons. Two peaks at δ 101.7 and 145.5 were assigned to C_α and C_β, respectively, of the vinylidene moiety. A sharp singlet at δ 5.1 in the ^{31}P NMR spectrum was assigned to Ir–PPh_3. The FAB mass spectrum showed a molecular ion at m/z 894 which fragmented by successive loss of eight CO ligands.

Spectroscopic data confirmed that complex **3** was also related to **1** by the addition of two hydrogens. The ^1H NMR spectrum contained a high field doublet at δ −23.48 [J(PH) 12 Hz] from a bridging hydride ligand. A characteristic low-field doublet at δ 7.81 [J(PH) 5 Hz] was found for the alkyne CH proton. The singlet at δ 112.5 in the $^{13}C\{^1H\}$ NMR spectrum was assigned to the =CH carbon with the aid of off-resonance decoupling; the resonance of the other carbon was in the aromatic region and could not be identified. The CO ligands resonated at δ 152.8 and 171.2 (Ir–CO) and at δ ca. 210 (Fe–CO). The FAB mass spectrum contained a molecular ion at m/z 894 and fragment ions formed by stepwise loss of eight CO ligands. These data are consistent with the formulation of **3** as the μ_3-alkyne complex, isomeric with **2**. Again, the proposed structure is that in which the formal π-bond is directed towards the least electron-rich metal atom, in this case one of the Fe atoms.

The formation of **3** probably occurs by addition of H^- to C_α of the phenylacetylide ligand in **1** to give an anionic intermediate, followed by addition of a proton to the metal framework. The ready 1,2-hydrogen shift which results in the isomerisation of **3** to **2** is a well-established reaction [4], and occurs almost quantitatively on heating **3** are refluxing toluene for 90 min.

Vahrenkamp and coworkers [4] have established the geometric changes occurring in the alkyne–vinylidene transformation on Co_2Ru systems. The CC bond gradually inclines with respect to the metal plane (alkyne, 1; acetylide, 19; vinylidene 50°). In the present work, we find the inclinations of the acetylide [1] and vinylidene ligands to be 18.6 and 65.5°, respectively, to the mean Fe_2Ir plane. These changes are consistent with the results of a theoretical study by Silvestre and Hoffmann [5].

(c) *Auration*. As mentioned above, the reaction **1** with Na/Hg or $K[BH(CHMeEt)_3]$ is believed to generate a hydrido-anion. Tetrahydrofuran solutions of this anion, generated using sodium amalgam, react readily with $[O\{Au(PPh_3)\}_3][BF_4]$ to give dark red solutions, from which the major product, $AuFe_2Ir(\mu_3\text{-}HC_2Ph)(CO)_8(PPh_3)_2$, **4**, was isolated by TLC. A small amount of the digold cluster $Au_2Fe_2Ir(\mu_4\text{-}C_2Ph)(CO)_7(PPh_3)_2$ (**5**) (see below) was also obtained.

Complex **4** was identified from microanalytical and spectroscopic data. The solution IR spectrum contained six terminal ν(CO) bands. The ^1H NMR spectrum contained resonances at δ 7.14–7.62, assigned to the phenyl groups. A characteristic low field signal found at δ 9.18 [d, J(PH) 13 Hz, 1H] was assigned to the CH proton of the μ_3-alkyne (cf. the similar resonance in $Co_2Ru(\mu_3\text{-}\eta^2\text{-}HC_2Ph)(CO)_9$ at δ 9.53 [4]). The multiplet between δ 126.0–135.0 in the $^{13}C\{^1H\}$ NMR spectrum, assigned to the phenyl groups, and probably including C_β of the alkyne, and the signal at δ 102.5 assigned to C_α of the alkyne, were the only resonances observed. The FAB mass spectrum contained a weak pseudo-molecular ion at m/z 1353 ($[M + H]^+$) which decomposed by the stepwise loss of eight CO groups and an $Au(PPh_3)$ fragment. The gold-containing ions at m/z 721 and m/z 459 were assigned to $[Au(PPh_3)_2]^+$ and $[Au(PPh_3)]^+$, respectively.

X-ray quality crystals of **4** could not be obtained, so that the precise position of the $Au(PPh_3)$ group has not been determined; the usual isolobal equivalence

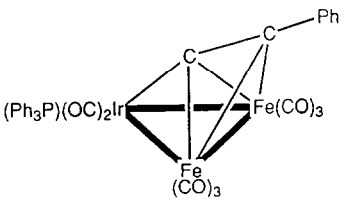

(1)

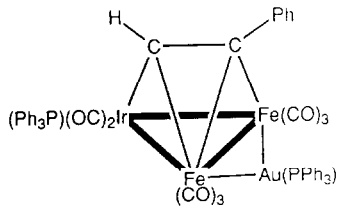

(4)

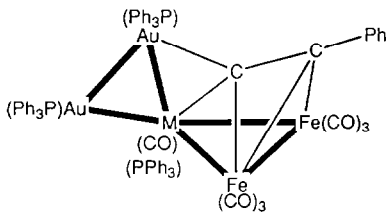

(5) M = Ir
(7) M = Rh

$H\overset{\mu}{\cdot}Au(PR_3)$ points to its bridging one edge of the Fe_2Ir triangle rather than adopting a μ_3 (capping) position.

Complex **4** was also obtained from the reaction of the anion of **1**, generated using either Na/Hg or $K[BH(CHMeEt)_3]$ in THF, and $AuCl(PPh_3)$; small amounts of **5** were also obtained. This observation supports the premise that initial nucleophilic attack of H^- occurs at C_α of the acetylide ligand in **1**. A similar reaction with $Fe_3(\mu_3\text{-}\eta^2\text{-}CN^tBu)(CO)_9$ has been described [6]. In this case, the cluster-bound isocyanide was found to add H^- to give $[Fe_3(\mu_3\text{-}\eta^2\text{-}HCN^tBu)(CO)_9]^-$, which could be protonated or aurated to give $Fe_3(\mu\text{-}H)(\mu_3\text{-}\eta^3\text{-}HCN^tBu)(CO)_9$ and $AuFe_3(\mu_3\text{-}\eta^2\text{-}HCN^tBu)(CO)_9(PPh_3)$, respectively.

The reaction of **1** with $K[HB(CHMeEt)_3]$ followed by addition of the trigold-oxonium reagent gave a number of additional products, one of which was identified as a CH_2Cl_2 solvate of $Au_3Fe_2Ir(C_2HPh)(CO)_7(PPh_3)_4$ (**6**). The ^1H NMR spectrum of **6** contains resonances between δ 7.0 and 7.5 (Ph) and a broad unresolved signal at δ 7.05, which we assign to a vinylidene proton (cf. δ 6.89 in $Co_2Ru(\mu_3\text{-}CCHPh)(CO)_9$ [4]). The FAB mass spectrum of **6** contained a molecular ion at m/z 2242 and ions related to this by successive loss of six CO groups and loss of PPh_3. Gold-containing ions were found at m/z 1377, 1115 and 721, assigned to $[Au_3(PPh_3)_3]^+$, $[Au_2(PPh_3)_2]^+$ and $[Au(PPh_3)_2]^+$, respectively. It is not surprising that a tris-gold adduct has been found given the nature of the aurating reagent used but the disposition of the three $Au(PPh_3)$ units in **6**, expected to form either an open or closed Au_3 array, is not known.

We have shown earlier [2] that reactions of $[O\{Au(PPh_3)\}_3][BF_4]$ with appropriate substrates, carried out in the presence of [ppn][X] (X = OAc, $Co(CO)_4$, for example), often result in the introduction of the $Au_2(PPh_3)_2$ ligand (or two $Au(PPh_3)$ units). Complex **5** was obtained in this way from **1** as orange crystals in 83% yield. The rhodium analogue **7** was prepared similarly. The complex

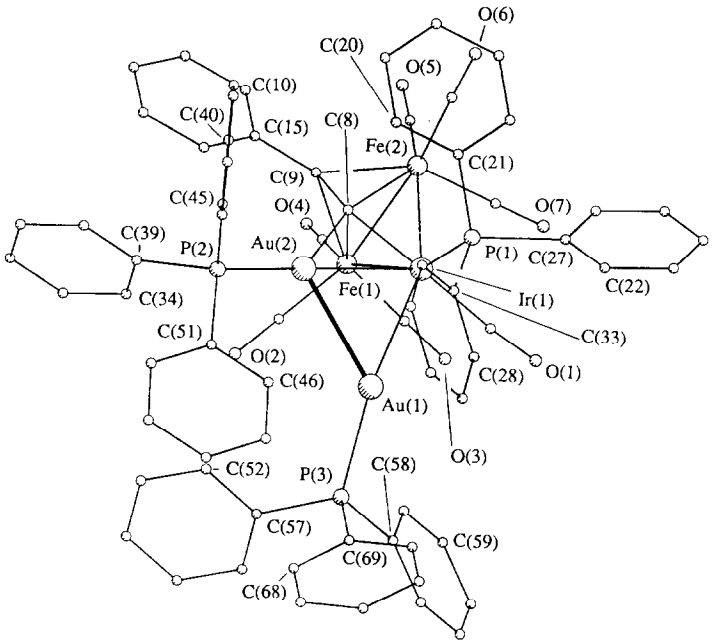

Fig. 2. Molecular structure and crystallographic numbering scheme for $Au_2Fe_2Ir(\mu_4\text{-}C_2Ph)(CO)_7(PPh_3)_3$ (**5**).

$AuCo(CO)_4(PPh_3)$ was also isolated from the reaction products. The formulations of **5** and **7** were indicated by microanalytical and FAB MS data, and the molecular structure of **5** was determined by X-ray methods.

Structure of $Au_2Fe_2Ir(\mu_4\text{-}\eta^2\text{-}C_2Ph)(CO)_7(PPh_3)_3$ *(5).* The molecular structure of **5** is shown in Fig. 2 and Table 2 collects significant bond distances and angles.

Table 2

Selected interatomic distances (Å) and angles (deg) in $Au_2Fe_2Ir(\mu_4\text{-}C_2Ph)(CO)_7(PPh_3)_3$ (**5**)

Au(1)–Au(2)	2.847(1)	Au(1)–Ir(1)	2.633(1)
Au(2)–Ir(1)	2.726(1)	Ir(1)–Fe(1)	2.709(3)
Ir(1)–Fe(2)	2.744(4)	Fe(1)–Fe(2)	2.501(5)
Ir(1)–P(1)	2.287(6)	Au(1)–P(3)	2.269(6)
Au(2)–P(2)	2.269(6)	Au(2)–C(8)	2.39(2)
Ir(1)–C(8)	1.96(2)	Fe(1)–C(8)	2.07(2)
Fe(2)–C(8)	2.08(2)	Fe(1)–C(9)	2.14(2)
Fe(2)–C(9)	2.06(2)	C(8)–C(9)	1.34(3)
Au(2)–Au(1)–P(3)	132.7(2)	Au(1)–Ir(1)–Fe(1)	90.3(1)
Au(2)–Au(1)–Ir(1)	59.5(1)	Au(2)–Ir(1)–Fe(2)	107.1(1)
Ir(1)–Au(1)–P(3)	166.0(2)	Au(2)–Ir(1)–Fe(1)	86.5(1)
Au(1)–Au(2)–Ir(1)	56.3(1)	Au(2)–C(8)–Ir(1)	77.0(7)
Au(1)–Au(2)–C(8)	91.2(6)	Au(2)–C(8)–C(9)	129(2)
Ir(1)–Au(2)–P(2)	170.0(2)	Ir(1)–C(8)–C(9)	151(2)
Au(1)–Ir(1)–Fe(2)	144.8(1)	Au(1)–Au(2)–P(2)	122.4(1)
Au(1)–Ir(1)–Au(2)	64.1(1)	C(8)–C(9)–C(15)	139(2)

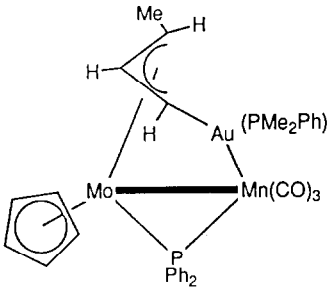

(8)

The structure of **5** is closely related to that of **1**, the major difference being the coordination of a $Au_2(PPh_3)_2$ unit to the Ir atom with an additional interaction between Au(2) and C(8) of the acetylide ligand. The cluster core comprises a *spiro* or 'bow-tie' arrangement of the five metal atoms with the two halves of the tie defined by the Ir(1)Fe(1)Fe(2) and Ir(1)Au(1)Au(2) triangles. The dihedral angle between the planes is 86.0°. The Ir–Fe [2.709(3), 2.744(4) Å], Fe–Fe [2.501(5) Å] and Ir–P(1) [2.287(6) Å] distances are all comparable to those found in complex **1**. The Au–Ir distances [Ir–Au(1) 2.633(1), Ir–Au(2) 2.726(1) Å] may be compared with the sum of the metallic radii (2.794 Å) and the Ir–Au(1) interaction falls within the range found for the analogous distance in other mixed-metal clusters (2.593–2.675 Å) [7]. In the anion $[AuFe_2Ir_2(\mu\text{-}CO)_3(CO)_9(PPh_3)]^-$, the $Au(PPh_3)$ group caps an $FeIr_2$ face, with Au–Fe 2.806(1), Au–Ir 2.797(1) and 2.829(1), and Fe–Ir 2.686(1) and 2.776(1) Å [3]. The coordination mode of the acetylide ligand in **3** can be described as distorted $\mu_4\text{-}\eta^2\text{-}(\perp)$ [8] with the angle between the C≡C axis and the bridged Fe(1)–Fe(2) vector being ca. 103°. The Ir–C_α [1.957(23) Å] and C≡C distances [1.340(31) Å] fall within the values found for $\mu_4\text{-}\eta^2\text{-}(\perp)$ acetylide ligands [8] and are comparable to those in **1**.

An interesting feature of the structure of **5** is the Au(2)–C(8) interaction [2.387(22) Å]. Gold–carbon interactions have been noted previously in the complexes $[(\eta\text{-}C_5H_5)Fe(\eta\text{-}C_5H_4)Au_2(PPh_3)_2][BF_4]$ [9], $[AuW_2(\mu\text{-}CC_6H_4Me\text{-}4)_2(CO)_4(\eta\text{-}C_5H_5)_2][PF_6]$ [10] and $[(\eta\text{-}C_5H_5)MoMn(\mu\text{-}PPh_2)\{\mu\text{-}\sigma : \eta^4\text{-}CH(Me)CHCHAu(PMe_2Ph)\}(CO)_4]$ (**8**) [11] where Au–C contacts of 2.16(3), 2.12(2) and 2.19(1) Å, respectively, were found. The latter complex is possibly the closest analogue to **5** and contains an η^3-CHMeCHCHAu(PMe_2Ph) ligand bridging the Mo–Mn bond. The $Au(PR_3)$ unit is considered to replace the agostic hydrogen found in the η^3-$CHMeCHCH_2$ analogue and to be involved in a similar type of bonding. The longer distance in **5** might be a result of steric interaction between the PPh_3 ligand on Ir, which is bonded *cis* to C_α of the acetylide ligands, and the $Au(PPh_3)$ group interacting with C_α.

In **5**, the seven CO groups are distributed three to each iron and one to the iridium. Although the least hindered site of attack on the iridium atom in **1** is the position occupied by CO(2), which is *trans* to C_α of the acetylide ligand, comparison of the two structures suggests that the $Au_2(PPh_3)_2$ unit occupies the position of CO(1), thus allowing interaction of the digold unit with C_α.

Spectroscopic data obtained for **5** and **7** were in accord with the determined structure. Their IR spectra were similar and contained only terminal ν(CO) bands. Multiplets, assigned to phenyl group resonances, were the only signals observed in their ^{1}H NMR spectra; the compounds proved too insoluble to obtain ^{13}C NMR spectra. The $^{31}P\{^1H\}$ NMR spectrum of **7** contained two broad singlets at δ 40.8 and 47.8 which were assigned to inequivalent $Au(PPh_3)$ groups; a sharp doublet at δ 52.6 in the spectrum of **7** was assigned to $Rh-PPh_3$ on the basis of the observed 141 Hz coupling to ^{103}Rh. By analogy the broad singlets at δ 42.8 and 47.6 and the sharp singlet at δ 30.6 in the $^{31}P\{^1H\}$ NMR spectrum of **5** were assigned to $Au-PPh_3$ and $Ir-PPh_3$, respectively. The FAB mass spectra of **5** and **7** contained weak pseudo-molecular ions at *m/z* 1794 and *m/z* 1694, respectively, corresponding to $[M + H]^+$ and $[M + 2H]^+$, respectively. These ions decomposed by successive loss of seven CO groups and an $Au(PPh_3)$ group. Both spectra contained strong ions at *m/z* 721 and 459 assigned to $[Au(PPh_3)_2]^+$ and $[Au(PPh_3)]^+$, respectively. An ion corresponding to $[\{Au_2(PPh_3)_2\}H]^+$ was also found in the FAB spectrum of **5** at *m/z* 919.

Various alternative routes to **5** were investigated. Little reaction was found between complex **1** and the trigold-oxonium reagent alone, so that direct addition of $Au_3(PPh_3)_3$ or stepwise addition of three $Au(PPh_3)$ groups to give **6** can probably be ruled out. The orange solution obtained from the reaction of the trigold-oxonium salt with $[ppn][Co(CO)_4]$ in THF also did not react with **1** to form **5**. For preparative purposes it was found that treatment of **1** with $[ppn][Co(CO)_4]/[O\{Au(PPh_3)\}_3][BF_4]$ was the best synthetic route (83%). Recently it has been found that [ppn] Cl or $[ppn][OAc]/[O\{Au(PPh_3)\}_3][BF_4]$ achieves the same results giving in the former case $AuCl(PPh_3)$ as a side product which can be recycled [12]. At present we favour initial formation of a trigold adduct of **1**, perhaps via an intermediate activated by the $[ppn]^+$ counter-anion, which is then degraded by the added nucleophile with loss of $[Au(PPh_3)]^+$.

The isolobal relationship between $Au(PPh_3)$ and H is of limited use in predicting structures of clusters containing more than one gold atom [13–15]. This is because of the propensity of gold to form Au–Au bonds. However, as we have pointed out previously, to a first approximation the digold unit $Au_2(PPh_3)_2$ is isolobal with H_2. Complex **5** may model the first stage of the reaction of dihydrogen with complex **1**. The formal addition of H_2 ($\equiv H^-/H^+$) to **1** was shown above to give initially the hydrido-alkyne cluster **3** which rearranged thermally to the hydrido-vinylidene cluster **2**. Similarly, hydrogenation of **1** gave **2** which we believe derives from **3** formed initially.

Formal substitution of a CO group in **1** by $Au_2(PPh_3)_2$ results in the formation of **5** (Scheme 3). Thus approach of the H_2 molecule with oxidative addition to the Ir centre is followed by migration of one H atom to bridge the Ir–Fe bond, and of the second to C_α. Although addition of H_2 to **1** gave the vinylidene **2**, the reaction conditions favour the isomerisation of the expected alkyne; addition of H^-/H^+ gave the latter, which on heating was converted to **2**. These reactions are summarised in Scheme 2.

A situation can be envisaged in which cleavage of the Au–Au bond and one of the Ir–Au bonds could give rise to structures **A** and **B** which are isolobal with **3** and **2**, respectively. However, no evidence has been found for the formation of complexes of this type in the pyrolysis or hydrogenation of complex **5**. No doubt this is

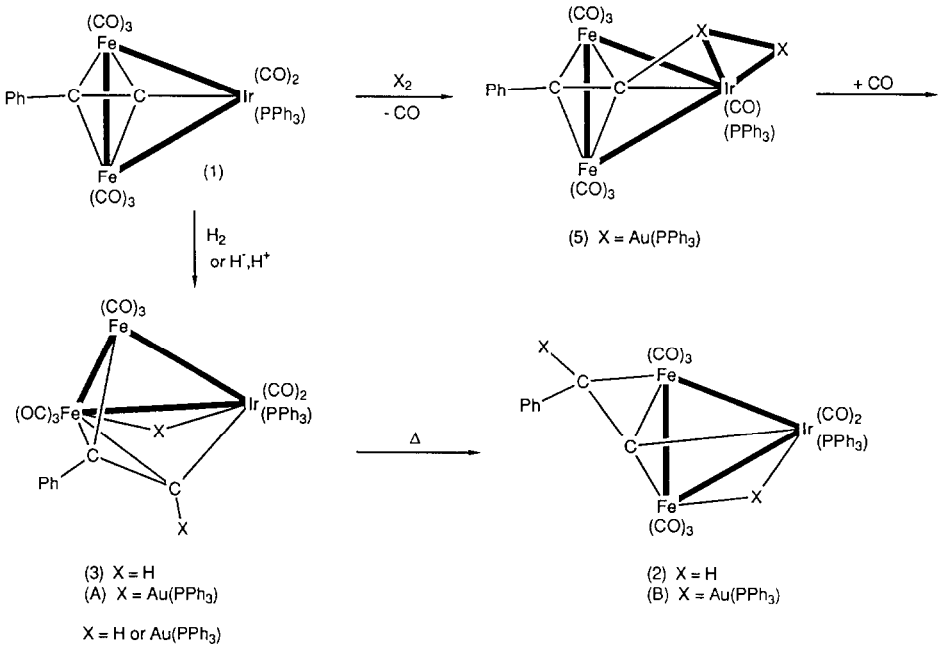

Scheme 2.

due to the tendency for formation and preservation of the Au–Au bond in **5**. A simple electron count requires the acetylide ligand to contribute 5e and the digold unit 2e to give an electron-precise count of 48 electrons for this cluster. The conversion of the acetylide ligand into the 4e donor depicted in **A** or **B** requires the addition of two electrons; this can be achieved by the addition of CO.

The principle which seems to govern construction of multi-Au(PR_3)-containing clusters is that the first unit occupies the position of H in the corresponding hydride cluster, if steric effects allow. Successive Au(PR_3) units then add to the least hindered triangular faces next to existing gold atoms. This leads to a compact arrangement of face-sharing tetrahedra with as many adjacent gold atoms as possible [7,14,15]. Thus, it is likely that complex **6** contains a $Au_3(PPh_3)_3$ ligand attached to the Fe_2Ir triangle on the opposite face to that occupied by the hydrocarbyl ligand.

Conclusions

Reduction of the bridging acetylide ligand in **1** was achieved by the stepwise addition of H^-/H^+ to give the isomeric hydrido-alkyne and hydrido-vinylidene clusters, $Fe_2Ir(\mu\text{-}H)(\mu_3\text{-}HC_2Ph)(CO)_8(PPh_3)$ and $Fe_2Ir(\mu\text{-}H)(\mu_3\text{-}CCHPh)(CO)_8(PPh_3)$. The vinylidene complex is also formed by the thermal isomerisation of the alkyne cluster, another example of the facile alkyne/vinylidene transformation on a cluster framework, or as one of the several products formed by direct hydrogenation of the acetylide cluster. The vinylidene cluster is structurally similar to the congeneric Co_2Fe and Co_2Ru μ_3-vinylidene clusters prepared by Vahrenkamp and coworkers [4] with the hydrocarbon moiety interacting in a distorted η^2-fashion with one of the less electron-rich metals present in the complex.

The acetylide cluster $Fe_2Ir(\mu_3\text{-}\eta^2\text{-}C_2Ph)(CO)_8(PPh_3)$ reacted with hydride or sodium amalgam to form an anionic species which could be aurated using $AuCl(PPh_3)$ or $[O\{Au(PPh_3)\}_3][BF_4]$ to give mono-, di- or tri-gold adducts. The unusual Au–C interaction present in the digold cluster $Au_2Fe_2Ir(\mu_4\text{-}\eta^2\text{-}C_2Ph)(CO)_7(PPh_3)_2$, best prepared from the reaction of the neutral acetylide cluster with $[O\{Au(PPh_3)\}_3][BF_4]$/ [ppn][$Co(CO)_4$], leads us to believe that the '$Au_2(PPh_3)_2$' unit may model an intermediate stage of addition of dihydrogen to the acetylide cluster.

Experimental

General experimental techniques were described in an earlier paper [16].

Starting materials. Literature methods were used to prepare $AuCl(PPh_3)$ [17], $[O\{Au(PPh_3)\}_3][BF_4]$ [17] and $Fe_2M(\mu_3\text{-}C_2Ph)(CO)_8(PPh_3)$ (M = Rh, Ir) [1].

A. *Reactions of $Fe_2Ir(\mu_3\text{-}C_2Ph)(CO)_8(PPh_3)$*

(a) With sodium amalgam. A solution of **1** (163 mg, 0.183 mmol) in THF (15 ml) was added to a freshly prepared sample of sodium amalgam (ca. 100 mg Na in 1.0 ml Hg) at −64 °C and stirred for 15 min. The dark red reaction mixture was warmed to 0 °C and stirred for a further 1 h. After standing for a period to allow the amalgam to settle, the solution was transferred by syringe to a Schlenk flask and filtered through Celite. The solution was then treated with H_3PO_4 (5 drops, excess) and stirred at 0 °C for 10 min. The dark red solution was evaporated to dryness, the residue extracted with CH_2Cl_2–water (25/10) and filtered through phase-separating paper. The organic layer was evaporated to dryness and the residue was separated by preparative TLC (acetone–CH_2Cl_2–light petroleum, 7/1/12) to give ten bands. Band 1 (R_f 0.67, red-pink) was crystallised (Et_2O/light petroleum) as red crystals of $Fe_2Ir(\mu\text{-}H)(\mu_3\text{-}\eta^2\text{-}CCHPh)(CO)_8(PPh_3)$ (**2**) (3 mg, 2%), identified by spot TLC and comparison of its IR ν(CO) spectrum with that of a sample prepared as below. Band 2 (R_f 0.61, orange-brown) crystallised (Et_2O/light petroleum) to give dark red crystals of $Fe_2Ir(\mu\text{-}H)(\mu_3\text{-}\eta^2\text{-}HC_2Ph)(CO)_8(PPh_3)$ (**3**) (77 mg, 47%), m.p. > 150 °C (dec.). [Found: C, 45.41; H, 2.56; *M* (mass spectrometry), 894.] $C_{34}H_{21}Fe_2IrO_8P$ calc.: C, 45.71; H, 2.48%; *M*, 894. IR (cyclohexane): ν(CO) 2076w, 2047s, 2023m, 2009vs, 1986m, 1970m, 1955w cm^{-1}. ^1H NMR ($CDCl_3$): δ 7.81 [d, *J*(PH) 5 Hz, 1H, CH]; 7.1–7.5 (m, 20H, Ph); −23.48 [d, *J*(PH) 12 Hz, 1H, Fe–H]. $^{13}C\{^1H\}$ NMR [$CDCl_3$, $Cr(acac)_3$]: δ 112.5 (s, H*C*CPh); 126.5–133.4 (m, Ph); 152.8 (s, Ir–CO); 171.2 (m, Ir–CO); 210.4, 212.1, 213.0 (3 × s, Fe–CO). FAB MS: 894, $[M]^+$, 19; 838, $[M - 2CO]^+$, 3; 810, $[M - 3CO]^+$, 100; 782, $[M - 4CO]^+$, 33; 754, $[M - 5CO]^+$, 19; 726, $[M - 6CO]^+$, 83; 698, $[M - 7CO]^+$, 13; 670 $[M - 8CO]^+$, 4. The remaining eight bands contained only trace amounts and were not identified.

(b) With K-Selectride, K[BH(CHMeEt)$_3$]. A solution of **1** (103 mg, 0.116 mmol) in THF (20 ml) at 0 °C was treated with $K[BH(CHMeEt)_3]$ (0.16 ml of a 1.0 mol L^{-1} solution in THF, 0.16 mmol), and stirred for 60 min. The now darkened solution was warmed to ambient temperature and H_3PO_4 (3 drops, excess) was added. After stirring for a further 10 min, the solution was evaporated to dryness and the residue extracted with equal volumes of CH_2Cl_2 and H_2O (10 ml). The organic layer was separated by filtration through phase-separating paper and then

evaporated to dryness. The residue was separated by preparative TLC (acetone–light petroleum, 1/4) giving twelve bands. Band 1 (R_f 0.92, red-pink) gave solid $Fe_2Ir(\mu\text{-}H)(\mu_3\text{-}\eta^2\text{-}CCHPh)(CO)_8(PPh_3)$ (**2**) (3 mg, 3%), identified by spot TLC and its IR ν(CO) spectrum. Band 2 (R_f 0.86, red-brown) was crystallised (Et_2O/light petroleum) to give dark red crystals of **3** (20 mg, 19%), identified by its IR ν(CO), ^1H NMR and FAB mass spectra. Band 3 (R_f 0.42, orange) was obtained as crystals (CH_2Cl_2/light petroleum) (2 mg) but was not identified. IR (cyclohexane): ν(CO) 2084m, 2052s, 2020m, 2010s, 1994m, 1981m, 1964w cm^{-1}.

(c) With dihydrogen. A solution of **1** (48 mg, 0.054 mmol) in cyclohexane (20 ml) was hydrogenated in an autoclave (30 atm, 80 °C, 7 h). The resulting brown suspension was filtered, the filtrate evaporated to dryness and the residue separated by preparative TLC (acetone–light petroleum, 1/4) to give eleven bands. Band 1 (R_f 0.97, red) gave solid $Fe_2Ir(\mu\text{-}H)(\mu_3\text{-}\eta^2\text{-}CCHPh)(CO)_8(PPh_3)$ **2** (1 mg, 2%), identified by spot TLC and its IR ν(CO) spectrum. Bands 3 and 4 (R_f's 0.75 and 0.68, respectively) contained trace amounts and were not identified. Band 5 (R_f 0.61, brown) was crystallised (CH_2Cl_2/pentane) to give unidentified brown needles (12 mg), m.p. > 150 °C (dec.) [Found: C, 42.08; H, 2.46.] IR (cyclohexane): ν(CO) 2064 m, 2043m, 2029s, 2009s, 1997m, 1970m, 1855m, 1820m cm^{-1}. ^1H NMR (CD_2Cl_2): δ −23.0 [s(br), 1H, MH]; 7.47 (m, 20H, Ph). Band 7 (R_f 0.50, yellow) (1 mg). IR (cyclohexane): ν(CO) 2053m, 2004(sh), 1999s, 1981w, 1802m, 1791m cm^{-1}. The remaining bands were present in trace amounts and were not identified.

(d) With sodium amalgam and $[O\{Au(PPh_3)\}_3][BF_4]$. A solution of **1** (55 mg, 0.062 mmol) in THF (10 ml) was added to a freshly prepared sample of sodium amalgam (ca. 100 mg Na in 1.0 ml Hg) and the mixture was stirred at ambient temperature for 1 h. The dark red solution was filtered through Celite, cooled to 0 °C and $[O\{Au(PPh_3)\}_3][BF_4]$ (92 mg, 0.062 mmol) was added. The mixture was warmed to ambient temperature and stirred for 1 h. Evaporation and preparative TLC (CH_2Cl_2–acetone–cyclohexane, 4/1/5) gave ten bands. Band 1 (R_f 0.76, red) was crystallised (CH_2Cl_2/light petroleum) to give dark red rosettes of $AuFe_2Ir(\mu_3\text{-}\eta^2\text{-}HC_2Ph)(CO)_8(PPh_3)_2$ (**4**) (20 mg, 24%), m.p. > 176 °C (dec.). [Found: C 45.82; H, 2.89; *M* (mass spectrometry) 1353. $C_{52}H_{36}AuFe_2IrO_8P_2$ calc.: C, 46.24; H, 2.61%; *M* 1352.] IR (CH_2Cl_2): ν(CO) 2040m, 2008(sh), 1999vs, 1985s, 1959m, 1923m cm^{-1}. ^1H NMR ($CDCl_3$): δ 7.14–7.62 (m, 35H, Ph); 9.18 [d, *J*(PH) 13 Hz, 1H, HC_2Ph]. $^{13}C\{^1H\}$ NMR ($CDCl_3$): δ 102.5 (s, $HCCPh$); 126.0–135.0 (m, Ph); no other carbon resonances were observed. FAB MS: 1353, $[M + H]^+$, 2; 1296, $[M - 2CO]^+$, 9; 1268, $[M - 3CO]^+$, 41; 1240, $[M - 4CO]^+$, 39; 1212, $[M - 5CO]^+$, 33; 1184, $[M - 6CO]^+$, 81; 1156, $[M - 7CO]^+$, 100; 1128, $[M - 8CO]^+$, 7; 1079, $[M - Au(C_6H_3)]^+$, 14; 894, $[(M + H) - Au(PPh_3)]^+$, 15; 721, $[Au(PPh_3)_2]^+$, 60; 459, $[Au(PPh_3)]^+$, 46. Band 5 (R_f 0.62, orange) was crystallised (CH_2Cl_2/light petroleum) to give orange crystals of **3** (14 mg, 15%), identified by comparison of its IR ν(CO) and FAB mass spectra with those of an authentic sample (below). The remaining bands were present in trace amounts and were not identified.

(e) With $K[BH(CHMeEt)_3]$ and $[O\{Au(PPh_3)\}_3][BF_4]$. A solution of **1** (50 mg, 0.056 mmol) in THF (10 ml) at −64 °C was treated with $K[BH(CHMeEt)_3]$ (0.1 ml of a 1.0 mol L^{-1} solution in THF, 0.1 mmol). After 5 min the red-brown solution was warmed to ambient temperature and stirred for 35 min, after which the darkened solution was cooled to −64 °C. $[O\{Au(PPh_3)\}_3][BF_4]$ (95 mg, 0.064 mmol) was added and the mixture warmed to ambient temperature. After stirring

for 30 min the solution was evaporated to dryness and the residue separated by preparative TLC (CH_2Cl_2–acetone–cyclohexane, 6/1/4) to give eight bands. Bands 1, 2 and 3 (R_f's 0.96, 0.93 and 0.90 respectively) contained only trace amounts and were not identified. Band 4 (R_f 0.86, black-brown) was further separated by preparative TLC (CH_2Cl_2–acetone–cyclohexane 6/1/4) into two bands. Band 4a (R_f 0.72, orange) was crystallised (CH_2Cl_2/MeOH) to give orange crystals of **5** (4 mg, 4%) which was identified by comparison of its IR ν(CO) and FAB mass spectra with those of an authentic sample. Band 4b (R_f 0.67, black) was crystallised (CH_2Cl_2/MeOH) to give black needles of $Au_3Fe_2Ir(C_2HPh)(CO)_7(PPh_3)_4$ **6** 24 mg, 19%), m.p. > 200 °C (dec.). [Found: C, 45.43; H, 2.82; *M* (mass spectrometry), 2242. $C_{87}H_{66}Au_3Fe_2IrO_7P_4 \cdot CH_2Cl_2$ calc.: C, 45.40; H, 2.90%; *M*, 2242. IR (CH_2Cl_2): ν(CO) 2024w, 1988s, 1962m, 1933m, 1918w, 1893w cm^{-1}, ^1H NMR ($CDCl_3$): δ 5.31 (s, CH_2Cl_2); 7.05 (br, C*H*Ph); 7.00–7.54 (m, Ph). FAB MS: 2242, $[M]^+$, 0.4; 2214, $[M - CO]^+$, 0.5; 2186 $[M - 2CO]^+$, 0.9; 2158, $[M - 3CO]^+$, 0.9; 2130, $[M - 4CO]^+$, 16; 2102 $[M - 5CO]^+$, 10; 2074, $[M - 6CO]^+$, 2; 2048, $[M - 7CO]^+$, 0.6; 1896, $[M - 3CO - PPh_3]^+$, 6; 1868, $[M - 4CO - PPh_3]^+$, 5; 1840, $[M - 5CO - PPh_3]^+$, 21; 1812, $[M - 6CO - PPh_3]^+$, 18; 1377, $[Au_3(PPh_3)_3]^+$, 62; 1115, $[Au_3(PPh_3)_2]^+$, 14; 721, $[Au(PPh_3)_2]^+$, 100.

(f) With sodium amalgam and AuCl(PPh$_3$). To a freshly prepared sample of sodium amalgam (ca. 180 mg Na in 1.0 ml of Hg) was added a solution of **1** (82 mg, 0.092 mmol) in THF (10 ml) and the mixture was stirred for 20 min. The dark red solution was transferred via syringe to a Schlenk flask and filtered through Celite into a solution of $AuCl(PPh_3)$ (50 mg, 0.101 mmol) in THF (10 ml) and stirred for 1 h. Evaporation and preparative TLC (acetone–light petroleum, 1/4) afforded eight bands. The major band (R_f 0.69, red-pink) was further separated by preparative TLC (CH_2Cl_2–acetone–cyclohexane, 6/1/4) to give a major band (R_f 0.72, red-pink) which was crystallised (CH_2Cl_2/heptane) to afford red crystals of **4** (30 mg, 24%), identified by comparison of IR ν(CO) and ^1H NMR spectra with those of an authentic sample. The remaining bands were present in trace amounts and were not identified.

(g) With K[BH(CHMeEt)$_3$] and AuCl(PPh$_3$). A solution of **1** (50 mg, 0.056 mmol) in THF (10 ml) was treated with $K[BH(CHMeEt)_3]$ (0.08 ml of 1 mol L^{-1} solution in THF, 0.08 mmol) and stirred for 1 h at ambient temperature. The solution was cooled to 0 °C and $AuCl(PPh_3)$ (40 mg, 0.081 mmol) was added followed by a gradual warming to ambient temperature. After stirring for 1 h, the mixture was evaporated to dryness and the residue separated by preparative TLC (acetone–light petroleum, 1/3) to give eleven bands. Band 1 (R_f 0.64, red-brown) gave solid **1** (10 mg, 20%); Band 3 (R_f 0.53, red-pink) gave solid **4** (9 mg, 15%); Band 7 (R_f 0.38, orange) gave solid **5** (15 mg, 19%); Band 8 (R_f 0.32, dark red-black) gave solid **6** (4 mg, 4%). These compounds were identified by comparison of their IR ν(CO) spectra and spot TLC behaviour with those of authentic samples. The remaining compounds were present in trace amounts and were not identified.

(h) With [O{Au(PPh$_3$)}$_3$][BF$_4$]. A solution of **1** (31 mg, 0.035 mmol) in THF (10 ml) was treated with $[O\{Au(PPh_3)\}_3][BF_4]$ (51 mg, 0.035 mmol) and the resulting suspension stirred for 24 h. The dark orange solution was evaporated to dryness and the residue separated by preparative TLC (acetone–light petroleum, 3.5/10) to give five bands. Bands 1 and 2 (R_f 0.88 and 0.85, respectively) contained trace amounts and were not identified. Band 3 (R_f 0.45, orange (was crystallised

(CH_2Cl_2/MeOH) to give orange crystals of **5** (15 mg, 24%), identified by comparison of its IR ν(CO) and FAB mass spectra with those of an authentic sample. The remaining compounds were present in trace amounts and were not identified.

B. *Syntheses of* $Au_2Fe_2M(\mu_4\text{-}C_2Ph)(CO)_7(PPh_3)_3$ *(M = Ir, Rh)*

(a) M = Ir. A solution of **1** (54 mg, 0.061 mmol) in THF (20 ml) at ambient temperature was treated successively with $[O\{Au(PPh_3)\}_3][BF_4]$ (90 mg, 0.061 mmol) and [ppn][$Co(CO)_4$] (45 mg, 0.063 mmol). After ca. 1 min the red-brown mixture cleared to an orange solution. Evaporation and preparative TLC (acetone–light petroleum, 3.5/10) afforded two bands. Band 1 (R_f 0.53, colourless) gave solid $AuCo(CO)_4(PPh_3)$ (35 mg, 91%), identified by comparison of its IR ν(CO) spectrum with that of an authentic sample [18]. Band 2 (R_f 0.17, orange) was crystallised (CH_2Cl_2/MeOH) to give orange crystals of $Au_2Fe_2Ir(\mu_4\text{-}\eta^2\text{-}C_2Ph)(CO)_7(PPh_3)_3$ **5** (90 mg, 83%), m.p. > 150 °C (dec.). [Found: C, 45.97; H, 2.74; *M* (mass spectrometry), 1784. $C_{69}H_{50}Au_2Fe_2IrO_7P_3$ calc.: C, 46.51; H, 2.83%; *M*, 1783.] IR (CH_2Cl_2): ν(CO) 2018m, 1978m, 1962m, 1885w, 1876(sh) cm^{-1}. ^1H NMR ($CDCl_3$): δ 7.33 (m, Ph). $^{13}C\{^1H\}$ NMR [$CDCl_3$, $Cr(acac)_3$]: δ 126.0–134.0 (m, Ph); 215.2 (m, Fe–CO). $^{31}P\{^1H\}$ NMR (CH_2Cl_2):δ 30.6 (s, Ir–PPh_3); 42.8 [s(br), Au–PPh_3]; 47.6 [s(br), Au–PPh_3]. FAB MS: 1784, $[M + H]^+$, 6; 1699, $[M - 3CO]^+$, 50; 1671, $[M - 4CO]^+$, 2; 1643, $[M - 5CO]^+$, 47; 1615, $[M - 6CO]^+$, 74; 1587 $[M - 7CO]^+$, 3; 1324, $[M - Au(PPh_3)]^+$, 5; 919, $[\{Au_2(PPh_3)_2\} + H]^+$, 12; 721, $[Au(PPh_3)_2]^+$, 100; 459, $[Au(PPh_3)]^+$, 53.

(b) M = Rh. A solution of $Fe_2Rh(\mu_3\text{-}C_2Ph)(CO)_8(PPh_3)$ (40 mg, 0.05 mmol) in THF (10 ml) at 20 °C was treated successively with $[O\{Au(PPh_3)\}_3][BF_4]$ (75 mg, 0.051 mmol) and [ppn][$Co(CO)_4$] (36 mg, 0.051 mmol). The initial dark red suspension cleared to a dark brown-black solution. Evaporation and preparative TLC (acetone–light petroleum, 1/2.5) afforded one major band (R_f 0.30, black) which was crystallised (CH_2Cl_2/MeOH) to give black crystals of $Au_2Fe_2Rh(\mu_4\text{-}\eta^2\text{-}C_2Ph)(CO)_7(PPh_3)_3$ (**8**) (68 mg, 80%), m.p. > 200 °C (dec.). [Found: C, 48.84; H, 2.94; *M* (mass spectrometry), 1964; $C_{69}H_{50}Au_2Fe_2O_7P_3Rh$ calc.: C, 48.16; H, 2.98%; *M* 1962.] IR (CH_2Cl_2): ν(CO) 2008s, 1981m, 1970s, 1954s, 1904w cm^{-1}. ^1H NMR ($CDCl_3$): δ 7.32 (m, Ph). $^{31}P\{^1H\}$ NMR (CH_2Cl_2): δ 40.8 [s(br), Au–PPh_3]; 47.8 [s(br), Au–PPh_3]; 52.6 [d, J(RhP) 141 Hz, Rh–PPh_3]. FAB MS: 1694, $[M + 2H]^+$, 4; 1609, $[M - 3CO]^+$, 17; 1524, $[M - 6CO]^+$, 28; 1496, $[M - 7CO]^+$, 13; 1234, $[M - Au(PPh_3)]^+$, 12; 721, $[Au(PPh_3)_2]^+$, 100; 459, $[Au(PPh_3)]^+$, 91.

C. *Hydrogenation of* $Fe_2Ir(\mu\text{-}H)(\mu_3\text{-}\eta^2\text{-}CCHPh)(CO)_8(PPh_3)$ *(2) and* $Fe_2Ir(\mu\text{-}H)(\mu_3\text{-}n^2\text{-}HC_2Ph)(CO)_8(PPh_3)$ *(3)*

Hydrogenation of **2**, under the same conditions as above resulted only in decomposition while the hydrogenation of **3** (20 mg, 0.022 mol) as above resulted in many bands (preparative TLC). One of the these was the brown complex obtained in A(c) above (5 mg) (spot TLC, IR ν(CO) spectrum).

D. *Pyrolysis of* $Fe_2Ir(\mu\text{-}H)(\mu_3\text{-}\eta^2\text{-}HC_2Ph)(CO)_8(PPh_3)$ *(3)*

A solution of **3** (42 mg, 0.047 mol) in toluene (15 ml) was heated at reflux for 1.5 h, after which time the reaction was adjudged complete (TLC). The burgundy coloured solution was evaporated to dryness and the residue separated by preparative TLC (acetone–light petroleum, 1/4) to give one major band (R_f 0.78, red).

Crystallisation (hexane) gave dark red crystals of $Fe_2Ir(\mu\text{-}H)(\eta_3\text{-}\eta^2\text{-}CCHPh)(CO)_8(PPh_3)$ **2** (35 mg, 83%) , m.p. > 200 °C (dec.). [Found: C, 44.99; H, 2.53; *M* (mass spectrometry), 894. $C_{34}H_{21}Fe_2IrO_8P$ calc.:C, 45.71; H, 2.48%; *M*, 894.] IR (cyclohexane): ν(CO) 2072m, 2045vs, 2022s, 2009vs, 1986s, 1971m, 1961w, 1954w cm^{-1}. ^1H NMR ($CDCl_3$): δ −17.959 [d, *J*(PH) 13 Hz, 0.5H, FeH]; −17.962 [d, *J*(PH) 13 Hz, 0.5H, FeH]; 6.93 (s, 1H, CC*H*Ph); 7.35 (m, 20H, Ph). $^{13}C\{^1H\}$ NMR [$CDCl_3$, $Cr(acac)_3$]: δ 101.7 (s, C*C*HPh); 126.0–134.0 (m, Ph); 145.5 (s, *C*CHPh); 170.2, 176.1 (s, 2 × Ir–CO); 209.8, 212.7, 214.0, 247.8 (m, Fe–CO). $^{31}P\{^1H\}$ NMR (CH_2Cl_2): δ 5.1 (s, PPh_3). FAB MS: 894, $[M]^+$, 5; 866, $[M - CO]^+$, 5; 810, $[M - 3CO]^+$, 89; 782, $[M - 4CO]^+$, 33; 754, $[M - 5CO]^+$, 22; 726, $[M - 6CO]^+$, 100; 698, $[M - 7CO]^+$, 70; 670, $[M - 8CO]^+$, 9.

Crystallography

Intensity data for **2** and **5** were measured at room temperature on an Enraf–Nonius CAD4F diffractometer fitted with graphite-monochromated Mo-K_α radiation, $\lambda = 0.7107$ Å, employing the ω–2θ scan technique. The data were corrected for Lorentz and polarisation effects and for absorption with the use of an analytical procedure [19]. Crystal data for each complex are listed in Table 3.

The structure of **2** was solved by interpretation of the Patterson synthesis and that of **5** by direct methods [20]; both were refined by full-matrix least-squares

Table 3

Crystal and refinement details for complexes **2** and **5**

Complex	**2**	**5**
Formula	$C_{34}H_{22}Fe_2IrO_8P \cdot CH_2Cl_2$	$C_{69}H_{50}Au_2Fe_2IrO_7P_3 \cdot EtOH$
M.W.	978.3	1828.0
Crystal system	triclinic	monoclinic
Space group	$P\bar{1}$	*Cc*
a, Å	13.155(4)	12.956(1)
b, Å	15.039(3)	26.604(4)
c, Å	11.354(2)	19.190(2)
α, deg	111.69(2)	90
β, deg	115.27(2)	97.14(1)
γ, deg	95.25(2)	90
U, Å^3	1802.5	6563.1
Z	2	4
D_c, g cm^{-3}	1.803	1.850
F(000)	952	3511
μ, cm^{-1}	46.64	69.87
Transmission factors, max/min	0.381, 0.191	0.340, 0.241
θ limits, deg	1.0–22.5	1.0–22.5
N_{meas}	5674	4508
N_{unique}	5674	4508
N_o, $I \geq 2.5\sigma(I)$	5261	3473
R	0.035	0.048
k	0.56	1.0
g	0.003	0.006
R_w	0.040	0.047

Table 4

Fractional atomic coordinates ($\times 10^5$ for Fe, Ir; $\times 10^4$ for remaining atoms) for $Fe_2Ir(\mu\text{-}H)(\mu_3\text{-}CCHPh)(CO)_8(PPh_3)\cdot CH_2Cl_2$ (**2**)

Atom	*x*	*y*	*z*
Ir	30536(1)	34729(1)	8578(2)
Fe(1)	7403(6)	26908(5)	−1620(8)
Fe(2)	18954(6)	44405(5)	20722(8)
P(1)	3811(1)	2101(1)	329(1)
C(1)	4444(5)	4317(4)	2635(7)
O(1)	5316(4)	4833(3)	3681(5)
C(2)	3367(5)	4083(4)	−237(7)
O(2)	3526(5)	4471(4)	−856(6)
C(3)	−145(5)	2874(5)	−1753(8)
O(3)	−722(5)	2967(5)	−2757(6)
C(4)	−349(5)	2769(4)	363(6)
O(4)	−1115(4)	2779(3)	591(5)
C(5)	412(5)	1365(5)	−923(8)
O(5)	115(5)	508(3)	−1403(9)
C(6)	3053(5)	5519(4)	3587(7)
O(6)	3793(5)	6250(3)	4578(6)
C(7)	1500(5)	4951(4)	794(7)
O(7)	1294(4)	5282(3)	2(5)
C(8)	875(5)	4747(4)	2708(6)
O(8)	260(4)	4964(3)	3165(6)
C(9)	2089(4)	3070(3)	1680(6)
C(10)	2380(4)	3411(3)	3148(5)
C(11)	1642(3)	3074(2)	3689(3)
C(12)	866(3)	2107(2)	2916(3)
C(13)	242(3)	1793(2)	3495(3)
C(14)	394(3)	2446(2)	4845(3)
C(15)	1170(3)	3413(2)	5618(3)
C(16)	1793(3)	3727(2)	5039(3)
C(17)	5421(3)	2505(3)	1332(4)
C(18)	6000(3)	3246(3)	1183(4)
C(19)	7227(3)	3607(3)	1968(4)
C(20)	7874(3)	3226(3)	2903(4)
C(21)	7295(3)	2485(3)	3052(4)
C(22)	6069(3)	2124(3)	2266(4)
C(23)	3386(3)	1172(2)	840(3)
C(24)	3549(3)	1502(2)	2246(3)
C(25)	3231(3)	814(2)	2673(3)
C(26)	2751(3)	−205(2)	1694(3)
C(27)	2588(3)	−535(2)	287(3)
C(28)	2906(3)	154(2)	−140(3)
C(29)	3450(3)	1356(3)	−1565(4)
C(30)	4174(3)	791(3)	−1853(4)
C(31)	3848(3)	147(3)	−3291(4)
C(32)	2797(3)	69(3)	−4442(4)
C(33)	2073(3)	634(3)	−4154(4)
C(34)	2399(3)	1278(3)	−2716(4)
C(35)	3924(10)	7376(8)	2218(12)
Cl(1)	5214(4)	6961(2)	2843(5)
Cl(2)	3718(4)	8087(3)	3508(4)

Table 5

Fractional atomic coordinates ($\times 10^5$ for Au, Ir; $\times 10^4$ for remaining atoms) for $Au_2Fe_2Ir(\mu_4\text{-}C_2Ph)(CO)_7(PPh_3)_3 \cdot EtOH$ (**5**)

Atom	x	y	z
Au(1)	22385(10)	64626(3)	29031(6)
Au(2)	727(1)	66169(3)	38390(7)
Ir(1)	24600(–)	71966(3)	38300(–)
Fe(1)	1271(3)	7805(1)	2926(2)
Fe(2)	1904(3)	8165(1)	4106(2)
P(1)	3113(5)	6805(2)	4851(3)
P(2)	−532(5)	6045(2)	3973(3)
P(3)	2282(5)	5955(2)	1957(3)
C(1)	3733(22)	7156(10)	3495(15)
O(1)	4540(16)	7182(7)	3299(12)
C(2)	498(18)	7401(9)	2337(13)
O(2)	−1(17)	7139(8)	1961(12)
C(3)	2371(2)	7816(9)	2514(14)
O(3)	3131(17)	7860(8)	2212(12)
C(4)	759(22)	8368(11)	2551(16)
O(4)	429(20)	8742(10)	2292(15)
C(5)	1569(23)	8770(13)	4003(18)
O(5)	1276(23)	9216(12)	3946(17)
C(6)	2149(24)	8181(13)	5060(18)
O(6)	2315(17)	8242(9)	5638(13)
C(7)	3215(19)	8244(10)	3944(14)
O(7)	4013(17)	8323(8)	3821(12)
C(8)	1096(18)	7496(8)	3896(11)
C(9)	431(18)	7883(8)	3812(10)
C(10)	−1012(10)	8481(5)	3852(8)
C(11)	−2068(10)	8576(5)	3871(8)
C(12)	−2762(10)	8176(5)	3885(8)
C(13)	−2401(10)	7682(5)	3879(8)
C(14)	−1346(10)	7588(5)	3860(8)
C(15)	−651(10)	7988(5)	3847(8)
C(16)	3190(9)	6940(5)	6300(7)
C(17)	2761(9)	7037(5)	6918(7)
C(18)	1699(9)	7137(5)	6891(7)
C(19)	1068(9)	7139(5)	6247(7)
C(20)	1497(9)	7041(5)	5630(7)
C(21)	2558(9)	6941(5)	5656(7)
C(22)	5238(11)	6562(5)	5357(8)
C(23)	6275(11)	6696(5)	5555(8)
C(24)	6574(11)	7199(5)	5544(8)
C(25)	5836(11)	7569(5)	5335(8)
C(26)	4800(11)	7435(5)	5137(8)
C(27)	4501(11)	6932(5)	5149(8)
C(28)	3703(11)	5887(5)	4328(7)
C(29)	3739(11)	5364(5)	4300(7)
C(30)	3183(11)	5077(5)	4735(7)
C(31)	2592(11)	5314(5)	5198(7)
C(32)	2556(11)	5838(5)	5227(7)
C(33)	3112(11)	6124(5)	4792(7)
C(34)	−1830(10)	6424(5)	2853(8)
C(35)	−2786(10)	6525(5)	2458(8)
C(36)	−3709(10)	6418(5)	2731(8)
C(37)	−3678(10)	6208(5)	3400(8)
C(38)	−2723(10)	6107(5)	3795(8)

Table 5 (continued)

Atom	x	y	z
C(39)	−1799(10)	6215(5)	3522(8)
C(40)	−914(11)	6393(5)	5250(8)
C(41)	−1048(11)	6356(5)	5958(8)
C(42)	−981(11)	5889(5)	6291(8)
C(43)	−778(11)	5459(5)	5916(8)
C(44)	−644(11)	5495(5)	5207(8)
C(45)	−712(11)	5963(5)	4874(8)
C(46)	763(10)	5272(5)	3636(7)
C(47)	992(10)	4786(5)	3431(7)
C(48)	190(10)	4442(5)	3253(7)
C(49)	−841(10)	4584(5)	3280(7)
C(50)	−1070(10)	5070(5)	3485(7)
C(51)	−268(10)	5414(5)	3664(7)
C(52)	129(11)	5928(5)	1646(7)
C(53)	−804(11)	5923(5)	1197(7)
C(54)	−792(11)	5913(5)	471(7)
C(55)	154(11)	5909(5)	194(7)
C(56)	1088(11)	5915(5)	643(7)
C(57)	1075(11)	5924(5)	1369(7)
C(58)	3226(12)	6716(6)	1344(9)
C(59)	3926(12)	6933(6)	936(9)
C(60)	4626(12)	6631(6)	630(9)
C(61)	4626(12)	6112(6)	732(9)
C(62)	3926(12)	5894(6)	1140(9)
C(63)	3226(12)	6196(6)	1446(9)
C(64)	3618(11)	5183(6)	2467(8)
C(65)	3902(11)	4682(6)	2589(8)
C(66)	3204(11)	4299(6)	2365(8)
C(67)	2222(11)	4416(6)	2019(8)
C(68)	1939(11)	4918(6)	1897(8)
C(69)	2637(11)	5301(6)	2121(8)
O(108)	6362(28)	4892(16)	465(21)
C(100)	6325(45)	4811(23)	1201(19)
C(101)	6608(25)	5128(14)	1862(18)

procedures based on F[20]. Phenyl rings were refined as hexagonal rigid groups with individual isotropic thermal parameters in both refinements. For **2**, non-phenyl, non-hydrogen atoms were refined with anisotropic thermal parameters, while for **5**, the Au, Fe, Ir, P, C(8) and C(9) atoms were refined with anisotropic thermal parameters. For both models a weighting scheme of the form $w = k/[\sigma^2(F) + g(F)^2]$ was included. At this stage of the refinement of **5**, several residual electron density peaks associated with the metal atom positions were noted. These were modelled successfully with 2% site occupancy factors, there being two residual peaks associated with each metal atom. In addition, a disordered ethanol molecule of crystallisation was located and refined with constrained C–C and C–O bond lengths of 1.53 and 1.45 Å, respectively. For **2** a solvent dichloromethane molecule of crystallization was included. Phenyl hydrogen atoms were included in the model at their calculated positions with a common isotropic thermal parameter. The inclusion of Friedel pairs in the data set enabled the determination of the absolute

configuration of the structure of **5** (R_g values 0.061 and 0.071, respectively for either hand [19]); the $C2/c$ space group for this compound is precluded by the lack of molecular symmetry in the complex.

Scattering factors for neutral Au, Fe and Ir (corrected for f and f'') were from ref. 21 while those for the remaining atoms were as incorporated in the SHELX76 programme [19]. Final refinement details are listed in Table 3, fractional atomic coordinates are given in Tables 4 and 5 and the numbering schemes employed are shown in Figs. 1 and 2 which were drawn with PLUTO [22]. All positional parameters (including disordered metal positions), thermal parameters, bond distances and angles and listings of the observed and calculated structure factors are available from the authors (ERTT).

References

1 Part LXVI: M.I. Bruce, G.A. Koutsantonis and E.R.T. Tiekink, J. Organomet. Chem., 407 (1991) 391.
2 M.I. Bruce, P.E. Corbin, P.A. Humphrey, G.A. Koutsantonis, M.J. Liddell and E.R.T. Tiekink, J. Chem. Soc., Chem. Commun., (1990) 674.
3 R. Della Pergola, L. Garlaschelli, F. Demartin, M. Manassero, N. Masciocchi and M. Sansoni, J. Chem. Soc., Dalton. Trans., (1990) 127.
4 E. Roland, W. Bernhardt and H. Vahrenkamp, Chem. Ber., 118 (1985) 2858.
5 J. Silvestre and R. Hoffmann, Helv. Chim. Acta, 68 (1985) 1461.
6 (a) M.I. Bruce and B.K. Nicholson, J. Chem. Soc., Dalton Trans., (1983) 2385; (b) M.I. Bruce and B.K. Nicholson, J. Organomet. Chem., 250 (1983) 627.
7 P. Braunstein and J. Rosé, Gold Bull., 18 (1985) 1.
8 P. Ewing and L.J. Farrugia, Organometallics, 8 (1989) 1246.
9 (a) V.G. Andrianov, Yu T. Struchkov and E.R. Rossinskaya, J. Chem. Soc., Chem. Commun, (1973) 338; (b) T.V. Baukova, Yu.L. Slovokhotov and Yu.T. Struchkov, J. Organomet. Chem., 221 (1981) 375.
10 M.R. Awang, G.A. Carriedo, J.A.K. Howard, K.A. Mead, I. Moore, C.M. Nunn and F.G.A. Stone, J. Chem. Soc., Chem. Commun., (1983) 964; G.A. Carriedo, J.A.K. Howard, F.G.A. Stone and M.J. Went, J. Chem. Soc., Dalton Trans., (1984) 2545.
11 A.D. Horton, M.J. Mays and M. McPartlin, J. Chem. Soc., Chem. Commun., (1987) 424.
12 M.I. Bruce and P.A. Humphrey, in preparation.
13 D.G. Evans and D.M.P. Mingos, J. Organomet. Chem., 232 (1982) 171.
14 M.I. Bruce and B.K. Nicholson, Organometallics, 3 (1984) 101.
15 I.D. Salter, Adv. Organomet. Chem., 29 (1989) 249.
16 M.I. Bruce, M.L. Williams, B.W. Skelton and A.H. White, J. Organomet. Chem., 369 (1989) 339.
17 M.I. Bruce, B.K. Nicholson and O. bin Shawkataly, Inorg. Synth., 26 (1989) 324.
18 C.E. Coffey, J. Lewis and R.S. Nyholm, J. Chem. Soc., (1964) 1741.
19 G.M. Sheldrick, SHELX76—Programme for Crystal Structure Determination, University of Cambridge, 1976.
20 G.M. Sheldrick, SHELXS86—Programme for the Automatic Solution of Crystal Structures, University of Göttingen, 1986.
21 J.A. Ibers and W.C. Hamilton, International Tables for X-ray Crystallography, Vol. 4, Kynoch Press, Birmingham, 1974.
22 W.D.S. Motherwell, PLUTO—Plotting Programme for Molecular Structures, University of Cambridge, 1978.